Size-Induced Transition from Magnetic Ordering to Kondo Behavior in (Ce,Al) Compounds

Y. Y. Chen,[1] Y. D. Yao,[1] C. R. Wang,[1] W. H. Li,[2] C. L. Chang,[3] T. K. Lee,[1] T. M. Hong,[4] J. C. Ho,[5] and S. F. Pan[1]

[1]*Institute of Physics, Academia Sinica, Taipei, Taiwan, Republic of China*
[2]*Department of Physics, National Central University, Chung-li, Taiwan, Republic of China*
[3]*Department of Physics, Tamkang University, Tamsui, Taiwan, Republic of China*
[4]*Department of Physics, National Tsing Hua University, Hsinchu, Taiwan, Republic of China*
[5]*Department of Physics, Wichita State University, Wichita, Kansas 67260*

(Received 1 September 1999)

Magnetic ordering and Kondo behavior coexist in three (Ce,Al)-based compounds: $CeAl_2$, Ce_3Al, and Ce_3Al_{11}. A common feature apparently independent of crystal structures also prevails in terms of the size-induced transition between these two magnetic phenomena. As the particle size is reduced to nanoscale, the specific heat anomaly associated with the magnetic ordering diminishes. Although the Kondo temperature also decreases, the entropy associated with Kondo anomaly exhibits a large increase. This results in an enhancement of the Kondo behavior and an increased coefficient γ of the linear term in specific heat. For example, in 80 Å $CeAl_2$ the extrapolated $r(0)$ reaches 9000 mJ mol Ce^{-1} K^{-2}.

PACS numbers: 75.30.Mb, 72.15.Qm, 75.40.Cx

In $Ce_{3-x}La_xAl_{11}$, Trinkl *et al.* [1] have shown that the suppression of magnetic order is accompanied by an enhancement of the single ion Kondo interaction by La substitution. Since the magnetic order suppression can also be induced by reducing particle size in, e.g., transition metals [2], it is of great interest to examine further the interplay between Kondo interaction and magnetic order through the size effect. Not surprisingly, point contacts, wires, and thin films have been the subject of Kondo effect studies [3–5]. However, they have quite different geometry and physical configuration from that of fine particles [6] as focused upon in the present calorimetric work on $CeAl_2$, Ce_3Al, and Ce_3Al_{11}.

The three (Ce,Al)-based compounds are known to be heavy fermion systems. In its bulk form, $CeAl_2$ has a cubic Laves structure. It undergoes an antiferromagnetic ordering at $T_N = 3.8$ K with $\gamma = 150$ mJ mol Ce^{-1} K^{-2} as the coefficient of its linear term in specific heat [7]. Ce_3Al exhibits a hexagonal Ni_3Sn structure, with $T_N = 2.5$ K and $\gamma = 200$ mJ mol Ce^{-1} K^{-2} [8]. In contrast, Ce_3Al_{11} having an orthorhombic La_3Al_{11} structure has a ferromagnetic transition at $T_C = 6.2$ K followed by an antiferromagnetic order at $T_N = 3.2$ K, below which $\gamma =$ 120 mJ mol Ce^{-1} K^{-2} [1]. Calorimetrically determined specific heat is a thermodynamic quantity providing the basis of entropy calculation in data analysis. However, one needs to take into consideration the large surface-to-volume ratio for nanoscale particles. This complication is compounded by the possible alteration of physical properties near the surface [9].

To fabricate $CeAl_2$, Ce_3Al, or Ce_3Al_{11} particles, the corresponding bulk compound was first prepared by arc melting thoroughly mixed constituent elements, Ce(99.9% pure) and Al(99.9999% pure), in argon. Structural confirmation was made using powder x-ray diffraction. Particle specimens were then fabricated on a liquid-nitrogen cold trap by flash evaporation of bulk ingots in a 0.1 torr of high-purity helium. According to x-ray diffraction patterns for $CeAl_2$, there was no change in structure between particles and parent bulk material, except a slight lattice expansion ($\approx$0.37%), some line broadening, and a trace of CeO_2 in nanoparticle specimens. Nevertheless, the characteristic reactivity of fine particles, along with the high oxidation susceptibility of Ce, could likely lead to a thin layer of CeO_2 on the surface. Indeed, a blurred anomaly around $2\theta = 28.6°$ in the diffraction pattern, which corresponds to the main (111) peak of CeO_2, suggests the presence of such an impurity, but at a level not exceeding 5%.

High resolution transmission electron microscopy (HRTEM) was employed to observe directly the crystalline structure. An example of the HRTEM images in the photograph attached to Fig. 2 reveals several well-crystallized particles having clear lattice arrays of $CeAl_2$. The strongest diffraction plane (220) with a lattice spacing of 2.85 Å is indicated by a pair of arrows for one spherical particle. No abnormal lattice spacing of CeO_2 at its rim is noticed. Based on TEM images, an average diameter for $CeAl_2$ particles was estimated to be 80 Å. The approximately spherical shape of these particles makes it straightforward in calculating the density of states at the Fermi level $D(\varepsilon_F)$ [10]. The same procedures were also followed to characterize bulk and particle specimens of Ce_3Al and Ce_3Al_{11}. No distinct difference from that of $CeAl_2$ was observed, except a slightly more CeO_2 was shown in Ce_3Al presumably due to its higher Ce content. The average particle sizes of Ce_3Al and Ce_3Al_{11} are estimated to be 200 Å and 100 Å, respectively. To help delineate different contributions to the total specific heat of $CeAl_2$, isostructural but nonmagnetic $LaAl_2$ in both bulk and particle forms were also prepared by the same method to provide the basic specific heat contribution from phonon excitations only.

Calorimetric measurements between 0.1 and 50 K were performed using a thermal-relaxation microcalorimeter in

 0031-9007/00/84(21)/4990(4)$15.00

a ^{3}He and a ^{3}He-^{4}He dilution refrigerator [11]. Each mg-size sample was prepared by lightly pressing fine powders together. It is of interest to note that the surface oxidation layer can actually prevent a given particle from making electronic contact with its neighbors, thus upholding finite size effects, if any.

The temperature dependence of specific heat for bulk $CeAl_2$ and $LaAl_2$ is shown in Fig. 1 as C/T versus T. This format allows entropy determination through a simple integration: $S = \int (C/T)\, dT$. For bulk $CeAl_2$ a well-defined peak reveals the previously known antiferromagnetic ordering at $T_N = 3.8$ K. We can account for the specific heat of bulk $CeAl_2$ by the contributions of the lattice phonons $C_{\rm ph}$, magnetic order C_m, and crystal field induced Schottky anomaly $C_{\rm cry}$. $C_{\rm ph}$ is assumed to be the same as that of the isostructural nonmagnetic compound $LaAl_2$ with a Debye temperature $\Theta_D = 325$ K. After $C_{\rm ph}$ subtraction the specific heat in the high temperature region is fitted well to a Schottky anomaly $C_{\rm cry}$ with $T_{\rm CF} = 110$ K. The entropy integrated from the remainder C_m saturates to $R \ln 2$ at $T \approx 17$ K as expected for the ground state doublet of Ce^{3+} ions (the inset to Fig. 1). These results are in good agreement with early reports [7,12]. At well below T_N, specific heat data are fitted to the equation $C = \gamma T + \alpha T^3$, where the T^3 term comes from antiferromagnetic spin waves. The resulting $\gamma \approx 150$ mJ mol Ce^{-1} K^{-2} is only about one-sixth of the theoretical $\gamma(0)$ value at $T = 0$ based on the equation $T_K = \pi R/6\gamma(0)$ for the Kondo temperature $T_K = 5$–6 K reported for bulk $CeAl_2$ [7]. According to Fisk *et al.* [13] the γ suppression comes from the partial quenching of the Kondo effect by the internal magnetic field generated as magnetic moments order below T_N.

The specific heat for 80 Å $CeAl_2$ and 80 Å $LaAl_2$ is shown in Fig. 2; no antiferromagnetic transition is present at 3.8 K in 80 Å $CeAl_2$, except that a minor bump there with entropy only about 1% of $R \ln 2$ might represent a small number of larger particles in the specimen. Instead, an anomaly at much lower temperatures is believed to be the Kondo term judging from discussions below. The reduction of antiferromagnetic transition can be understood from a finite size effect. When the particle diameter becomes too small, the coherence length of the spin fluctuations can reach a point not large enough to sustain a true phase transition, as observed by Johnson *et al.* in Tb [14]. In resolving the total specific heat to various components, the lattice contribution is estimated from measurements on 80 Å $LaAl_2$, which yield a $\Theta_D = 212$ K by fitting the specific heat data to the theoretical model for a small particle with a free surface [11]. This Debye temperature is much smaller than that of bulk material, as anticipated for a lattice softening commonly observed in fine particles. A crystal field term with $T_{\rm CF} = 130$ K is also needed to fit the higher temperature data after having the lattice phonon subtracted. The nearly 20% higher $T_{\rm CF}$ value is presumably a consequence of the larger distance of Ce^{3+} ions as evidenced by the 0.37% lattice expansion based on the x-ray diffraction. This is qualitatively consistent with earlier pressurized resistivity measurements on $CeAl_2$ by Nicolas-Francillon *et al.* [12]. Quantitatively, however, the best fit requires only 0.7 mole of the Ce^{3+} ions in the compound contributing to this crystal field term. This is corroborated by a complementary SQUID measurement. The magnetic susceptibility for 80 Å $CeAl_2$ between 7 and 15 K roughly follows the Curie-Weiss law, yielding a Curie constant of 0.25 K emu mol Ce^{-1}, which is

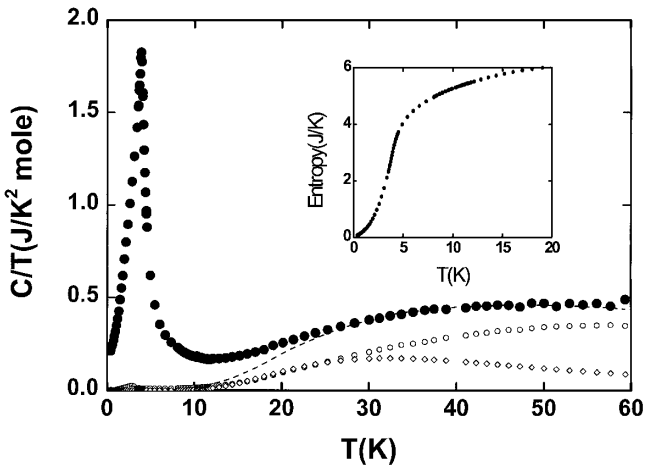

FIG. 1. Temperature dependence of specific heat, in terms of C/T versus T, for bulk $CeAl_2$ (closed circles). The phonon contribution $C_{\rm ph}$ is assumed to be the same as that for bulk $LaAl_2$ (open circles, showing a small superconducting-transition peak at 3.2 K). The dashed line represents the sum of $C_{\rm ph}$ and $C_{\rm cry}$ (diamonds). Inset: Integrated entropy $S = \int [(C - C_{\rm ph} - C_{\rm cry})/T]\, dT$.

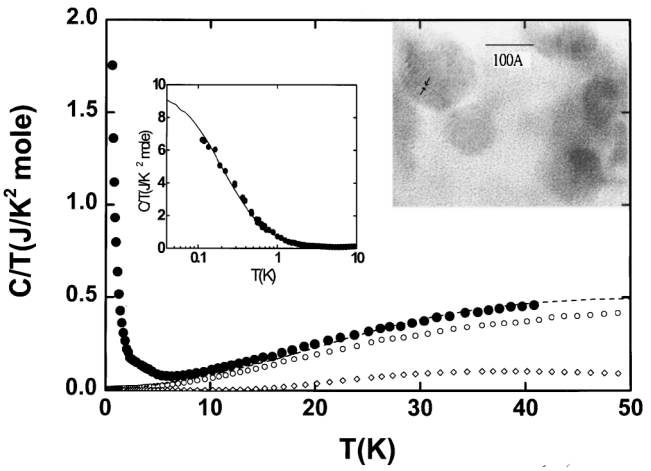

FIG. 2. Temperature dependence of specific heat, in terms of C/T versus T, for 80 Å $CeAl_2$ (closed circles, with the photograph showing an HRTEM image). The phonon contribution $C_{\rm ph}$ is assumed to be the same as that for 80 Å $LaAl_2$ (open circles). The dashed line represents the sum of $C_{\rm ph}$ and $C_{\rm cry}$ (diamonds). Inset: Lower temperature (C-$C_{\rm ph}$-$C_{\rm cry}$) values being fitted to the Kondo ion ($J = 1/2$) model with $T_K = 0.65$ K.

equivalent to the bulk value for 0.7 mole of Ce^{3+}. This consequence reveals a much larger fraction of Ce ions in 80 Å $CeAl_2$ to be tetravalent and hence nonmagnetic. A preliminary x-ray absorption experiment using synchrotron radiation also found a much larger fraction of Ce^{+4} ions. The major portion of the nonmagnetic Ce ions might be related then to the appreciable number of surface or outer-shell ions in a particle. For example, with a thickness of $0.5a_0$ (lattice parameter $a_0 = 8.09$ Å), the surface ions for 80 Å $CeAl_2$ would occupy ≈27% of the total volume.

To ascertain that the lower temperature anomaly for 80 Å $CeAl_2$ is of the Kondo origin, further calorimetric measurements were made in external magnetic fields H from 0.5 up to 7 T. The results with $H = 2.6$ and 6.5 T, respectively, are given in Fig. 3. If the anomaly were caused by an antiferromagnetic transition as seen in the bulk compound, an applied field would lower the ordering temperature. Instead, the anomaly actually moves up in temperature as the field increases. The profile of the anomaly and its response to magnetic fields are similar to the theoretical curves for a bulk Kondo ion ($J = 1/2$) derived by Sacramento [15] for bulk $CeAl_2$, except that the peak positions occur at slightly higher temperatures. It needs to be noted that a reduction factor of 0.7 is applied to the theoretical curves for the reasons mentioned above.

A closer examination of the zero-field data provides more insight of the heavy fermion behavior of the particles. After having the lattice and Schottky contributions subtracted at the lowest temperatures, the specific heat data of 80 Å $CeAl_2$ can be fitted to the Kondo model with $J = 1/2$ and $T_K = 0.65$ K (see Fig. 2 inset). Again, its integrated entropy is only 70% of $R\ln 2$. The significant reduction in T_K as compared to the bulk value of 5–6 K can be attributed only partially to lattice expansion. A relevant measure is the Gruneisen parameter for T_K [16]:

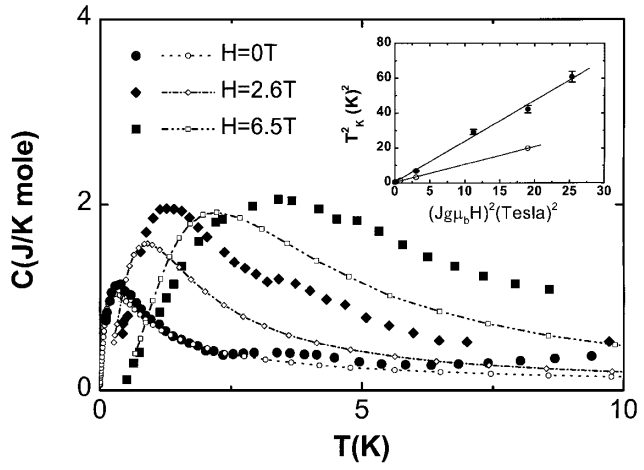

FIG. 3. Comparison for 80 Å $CeAl_2$ between the field-dependent specific heat data (solid symbols) and Kondo model calculations with $T_K = 0.65$ K (open symbols with lines). Inset: Field dependence of T_K from experimental data (solid circles) and Kondo model (open circles).

$$\Omega = -\left(\frac{V}{T_K}\right)\left(\frac{dT_K}{dV}\right). \quad (1)$$

Taking the value $\Omega = 30$–50 from Panfilov *et al.* [17] and the magnitude of $dV/V = 0.011$ from x-ray diffraction data, the estimated T_K for 80 Å $CeAl_2$ would be lowered to 2–4 K. The major difference to the experimental results must be caused, therefore, by the possible particle size and surface effects on the Kondo temperature. There is yet a complete theory about the Kondo effect in nanoparticles. Recent works [18,19] on Kondo impurities in thin films and wires indicate that surface-induced anisotropy for magnetic ions will influence the Kondo behavior. Kondo scattering depends on positions of the Ce ions from surface. Hence the Kondo lattice coherent temperature is likely to be reduced in nanoparticles. Subsequently antiferromagnetic transition which occurs below the Kondo coherence temperature is also suppressed. The particle size and surface effects may also play a role in the field measurement data. The peak temperature T_p of the Kondo anomaly increases from below 0.7 to 4 K as the magnetic field increases from 0 to 7 T. In the presence of magnetic field, the formation of Kondo singlets will be deterred, thus diminishing the heavy fermion characteristics, i.e., the large linear temperature coefficient of specific heat. This is reflected in the field dependence of the Kondo temperature for $Jg\mu_BH < T_K(0)$ [20]:

$$T_K^2(H) = T_K(0)^2 + (Jg\mu_BH)^2, \quad (2)$$

where J and g denote the total angular momentum and the Lande g factor of f electrons, respectively, and μ_B is the Bohr magneton. Since $T_K(H) \approx 2T_{\text{peak}}(H)$, we extracted $T_K(H)$ from magnetic field data and plotted it as $T_K^2(H)$ versus $(Jg\mu_BH)^2$ in the Fig. 3 inset. For 80 Å $CeAl_2$ the observed linear dependence of $T_K^2(H)$ versus H^2 can be considered as conforming well with the theoretical Kondo model, but the enhanced slope or proportionality constant 2.3 is much larger than the unity for bulk materials. The different response of Kondo temperature to magnetic field could then be attributed to the consequence of the size effect in small particles.

The most impressive finding of this work is the magnitude of the coefficient γ of the linear term in specific heat. At zero field, this parameter has already reached a quite large value of almost 7000 mJ mol Ce^{-1} K^{-2} at $T = 0.11$ K, the lowest temperature of measurements. It is extrapolated to 9000 mJ mol Ce^{-1} K^{-2} at absolute zero, which falls in the highest range ever reported for heavy fermion systems. If there are indeed only 70% of Ce ions responsible for the Kondo effect, one could even argue that the effective $\gamma(0)$ would be close to 13 000 mJ mol Ce^{-1} K^{-2}.

Similar temperature dependence of specific heat is obtained for the other two (Ce,Al) compounds Ce_3Al and Ce_3Al_{11} as shown in Fig. 4. In bulk form, they exhibit magnetic transitions at the expected ordering

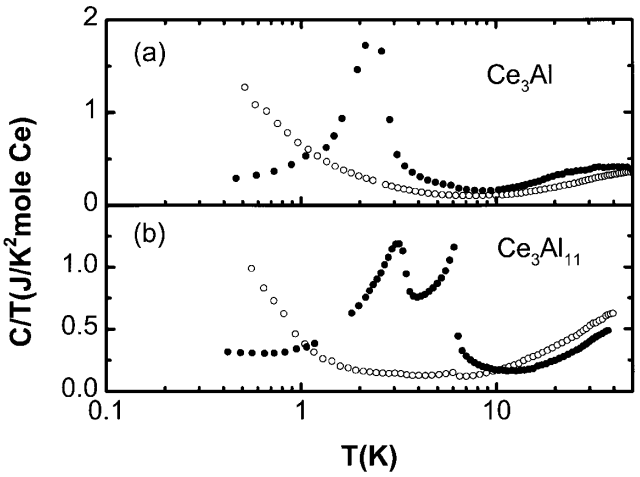

FIG. 4. Temperature dependence of specific heat for (a) bulk (closed circles) and 200 Å Ce_3Al (open circles) and (b) bulk (closed circles) and 100 Å Ce_3Al_{11} (open circles).

temperature T_N or T_C. In clear contrast, for 200 Å Ce_3Al or 100 Å Ce_3Al_{11} only residue bumps remain at these temperatures, indicating the almost total disappearance of magnetic ordering in these fine particles. Meanwhile, the Kondo anomalies are much enhanced, yielding large γ values of 1200 mJ mol Ce^{-1} K^{-2} for Ce_3Al and 1300 mJ mol Ce^{-1} K^{-2} for Ce_3Al_{11} at 0.5 K.

In conclusion, experimental observations in three (Ce,Al) compounds of different crystal structures show a general trend of a crossover from magnetic ordering to an enhanced Kondo behavior, possibly a consequence of particle size and surface effects. Since the interplay between Kondo interaction and magnetic order through the size and surface effects is yet to be fully understood, such revealing experimental results should lay the groundwork for a better theoretical development and models screening.

We are thankful for the help from HRTEM Lab in Materials Science Center, National Tsing-hua University. This work was supported by the National Council of the Republic of China under Grants No. NSC89-2112-M-001-031 and No. NSC89-2112-M-007-025.

[1] W. Trinkl, S. Corsepius, and G. R. Stewart, J. Alloys Compd. **46–49**, 239 (1996).
[2] J. L. Moran-Lopez and J. M. Sanchez, *New Trends in Magnetism, Magnetic Materials, and Their Application* (Plenum Press, New York, 1994).
[3] G. Chen and N. Giordano, Phys. Rev. Lett. **66**, 209 (1991).
[4] I. K. Yanson, V. V. Fisun, R. Hesper, A. V. Khotkevich, J. M. Krans, J. A. Mydosh, and J. M. van Ruitenbeek, Phys. Rev. Lett. **74**, 302 (1995).
[5] V. Chandrasekhar, P. Santhanam, N. A. Penebre, R. A. Webb, H. Vloeberghs, C. Van Haesendonck, and Y. Bruynseraede, Phys. Rev. Lett. **72**, 2053 (1994).
[6] G. Bergmann, Phys. Rev. Lett. **67**, 2545 (1991).
[7] F. Steglich, C. D. Bredl, M. Loewenhaupt, and K. D. Schotte, J. Phys. (Paris), Colloq. **40**, C5-301 (1979), and references therein.
[8] Y. Y. Chen, Y. D. Yao, B. C. Hu, C. H. Jang, J. M. Lawrence, H. Huang, and W. H. Li, Phys. Rev. B **55**, 5937 (1997).
[9] R. H. Kodama, A. E. Berkowitz, E. J. McNiff, Jr., and S. Foner, Phys. Rev. Lett. **77**, 394 (1996).
[10] W. P. Halperin, Rev. Mod. Phys. **58**, 533 (1986).
[11] Y. Y. Chen, Y. D. Yao, S. S. Hsiao, S. U. Jen, B. T. Lin, H. M. Lin, and C. Y. Tung, Phys. Rev. B **52**, 9364 (1995).
[12] M. Nicolas-Francillon, A. Percheron, J. C. Achard, O. Gorochov, B. Cornut, D. Jerome, and B. Coqblin, Solid State Commun. **11**, 845 (1972).
[13] Z. Fisk, J. L. Sarrao, J. L. Smith, and J. D. Thompson, Proc. Natl. Acad. Sci. U.S.A. **92**, 6663–6667 (1995).
[14] D. Johnson, P. Perera, and M. J. O'Shea, J. Appl. Phys. **79**, 5299 (1996).
[15] P. D. Sacramento and P. Schlottmann, Phys. Rev. B **40**, 431 (1989).
[16] J. D. Thompson and J. M. Lawrence, Handb. Phys. Chem. Rare Earths **19**, 383 (1994).
[17] A. S. Panfilov, I. V. Svechkarev, and E. Fawcett, Int. J. Mod. Phys. **7**, 703 (1993).
[18] V. M. Fomin, V. N. Gladilin, J. T. Devreese, C. Van Haesendonck, and G. Neuttiens, Solid State Commun. **106**, 293 (1998).
[19] O. Ujsaghy and A. Zawadowski, Phys. Rev. B **57**, 11 609 (1998).
[20] T. M. Hong and G. A. Gehring, Phys. Rev. B **46**, 231 (1992).